Correlation between Measured and Calculated Solar Radiation Data in Compiègne, France

E. ANTALUCA, L. MERINO, B. BECKERS,
Avenues - Urban Systems Engineering Department
Compiègne University of Technology
Compiègne
FRANCE
eduard.antaluca@utc.fr, luis-enrique.merino-quilodran@utc.fr, benoit.beckers@utc.fr
http://www.utc.fr http://www.heliodon.net

Abstract: - Heliodon software has been developed and used as a decision tool of designing with daylight availability by architects and urban designers. The present calculation algorithm of solar radiation of Heliodon is based only on the direct component of the solar radiation corresponding to clear sky days. In order to provide realistic simulations of the energy balance in the cities, the influence of the clouds needs to be taken into consideration. This article is a preliminary work in order to obtain a robust method to correlate the experimental data with the results obtained with the program Heliodon, for the city of Compiègne, France.

Key-Words: solar radiation modeling, daylight design, sky model

1 Introduction

Nowadays almost 50% of the world population lives in the cities and according to UN studies they will exceed 60% in 2030. So the cities will grow up and they will need more and more energy. Today, more than 3% of the land surface of our planet is covered by streets and urban areas. Moreover, for a number of urban areas it will be physically impossible to increase due to objective reasons. So the densification is the only available solution [1, 2].

In these conditions, in the design process, the consideration of natural light will improve the energy balance of buildings and minimize the negative impact of the cities on the environment. It becomes a fundamental requisite for architects and urban designers. In the near future, solar radiation studies will be extended to large urban areas. The collaboration between geographers, climatologists and physicists will be crucial in order to define the appropriate numerical and modeling approaches at different scales.

Sun is not only the source of life on earth but also an important source of energy. The total amount of energy emitted from the sun and reaching earth's surface is about 1.2×10^5 TW (3.6×10^4 TW on land). Total worldwide energy consumption in 2008 was about 15 TW with more than 80% derived from the combustion of fossil fuels. The amount of renewable energy (geothermal, wind, solar) was only 0.16 TW.

In the proper design of buildings and/or other systems with the energy of the sun, solar radiations models conform to reality are required. Extraterrestrial solar radiation can be described, in a deterministic way, for any space and time position on earth, as a function of the sun-earth distance, the earth's inclination and the sun's zenith angle. The ground-level solar radiation is attenuated by atmosphere conditions, clouds distribution, climate type etc. So, for a given constant spatiotemporal position, the ground-level radiation is very difficult to predict. However, some statistical approximations for a specific period of the year can be carried out.

In a preliminary research, the purpose of this work is a preliminary search to find a method to approximate the ground-level solar radiation for a given space position on earth, during a specific period, using a deterministic solar radiation computation and available experimental data.

2 Experimental data

Experimental data were recorded every five minutes from November 2008 to October 2009 at Compiègne, France using a SMA pyranometer (Fig. 1). Compiègne is located at 75 km (North) from Paris, France (49°24'54" North latitude and 2°49'23" East longitude). Its elevation is between 31 and 134 meters over mean sea level.

Fig. 1: The SMA pyranometer

The pyranometer was placed on the upper face of a solar panel system, inclined 30° from the horizontal and oriented to the south (Fig. 2). The sensitivity of the pyranometer is from 0 – 1500 W/m^2.

Fig. 2: Renewable Energy Station at Compiègne University of Technology [3]

The device measures the global radiation flux, H_c per square meter. It is the sum of the direct and diffuse radiation fluxes coming from the clear part of the sky and the diffuse radiation flux coming from its cloudy part. As an example, the one day data variation of H_c, measured in W/m^2, is presented on Fig. 3.

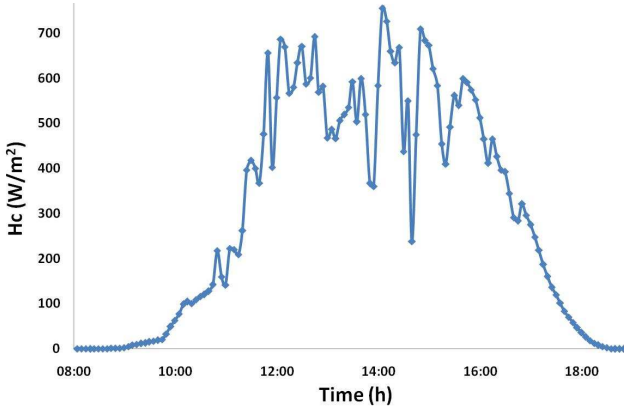

Fig. 3: Measured H_c on 008-11-03

The global radiation energy is the amount of the solar flux that is received by a surface in a specific time interval. Daily global radiation energy per unit area, E, is given by time integration of global radiation per unit area from sunrise to sunset (1) [4].

$$E = \int_{sunrise}^{sunset} H_c\,(t)\,dt \qquad (1)$$

The integration of the daily global radiation energy was simplified by considering the irradiance constant 2.5 minutes before and 2.5 after recording (Fig. 4).

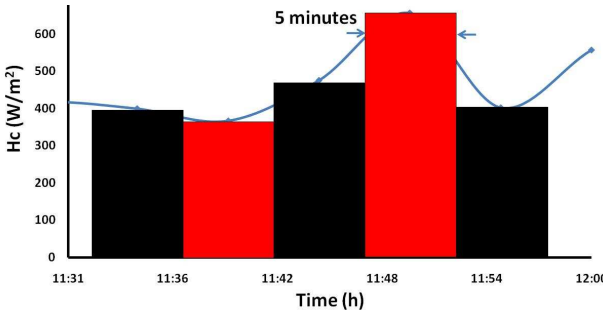

Fig. 4: Zoom on the integration simplification

Hence, the daily energy per unit area was obtained directly in kwh/m^2 using equation (2),

$$E = \frac{\Delta T}{60\,000}\sum_{i}^{n} H_{c_i} \qquad (2)$$

where ΔT=5 minutes and n is the total number of available recorded data for one day. The monthly global solar radiation energy per unit area is obtained as the sum of all the daily values over all the month (Fig.5).

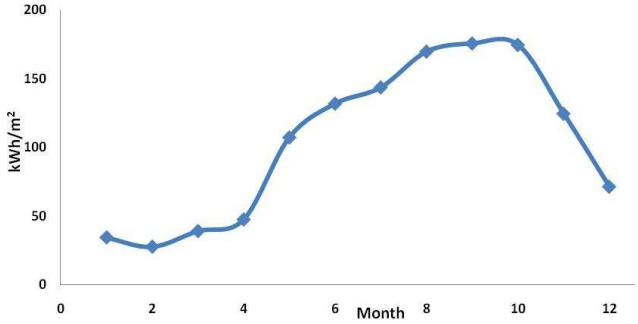

Fig. 5: The variation of the measured solar energy per unit area from November 2008 to October 2009

3 Heliodon simulation

Heliodon software (authors: B. Beckers & L. Masset) was developed to be used as a design tool by architects and urban designers [5]. Heliodon allows the computation of the direct solar radiation using stereographical and other geometrical projections, with respect to the real urban situation (time, space and masks) [6, 7].

In the present version, only the direct component of solar radiation is considered, using a model based on extraterrestrial solar radiation determined by the time and space position of the calculation point on earth. As explained in Campbell & Norman [8], Liu & Jordan [9] proposed a simple formula for the solar flux arriving at a point on the earth's surface:

$$H_c = H_0 \cdot \tau^m \qquad (3)$$

where H_0 is the extraterrestrial solar flux, τ is the atmospheric transmittance and m is the fraction between the real distance and the zenithal one. Typical values are: $H_0 = 1380\ W/m^2$, $\tau = 0.7$, m is given by the equation (4):

$$m = \frac{p_a}{101.3 \cdot \cos\psi} \qquad (4)$$

where p_a is the atmospheric pressure and ψ the zenithal angle. The atmospheric pressure is a function of altitude:

$$p_a = 101.3 \cdot e^{\frac{-altitude}{8.2}} \qquad (5)$$

In the equation (5) the altitude is expressed in km. The zenithal angle ψ is a function of the space position on earth and time for the computation point. The flux energy (in kwh/m^2) is obtained by time integration. The integration period can be varied between a few hours to the full year.

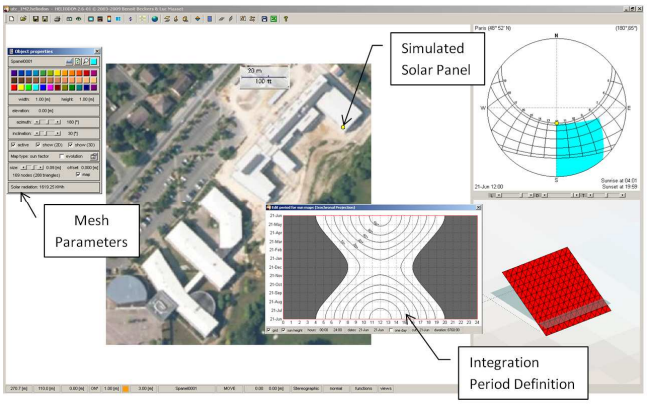

Fig. 6: Heliodon Model

A solar panel of one square meter was simulated in Heliodon. The simulation was performed using Compiègne (France) latitude and the panel was oriented to the south (Fig.6). The simulations have been carried out for different angles of inclination and different days of the year in order to be compared with the experimental data. The results are discussed in the next section.

4 Results and discussion

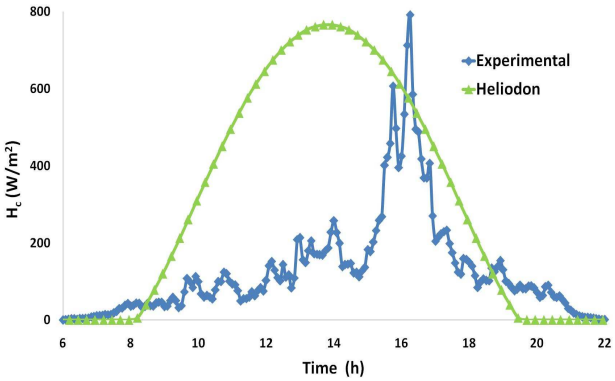

Fig. 7: Comparison between experimental and Heliodon data for a cloudy day

The solar radiation per unit area measurements are strongly affected by clouds. A comparison between the Heliodon data and the measurements for a cloudy day is presented on the Fig. 7. It can be seen that the difference between two series of data is very important. In order to make the same comparison for a sunny day, the variation of the daily global radiation energy was plotted to find the sunny days of every month. An example of this kind of plot is presented on Fig. 8 for the last two decades of May 2009. It is obvious from the plot that the maximum solar radiation energy was received by the solar panel on 30th of May.

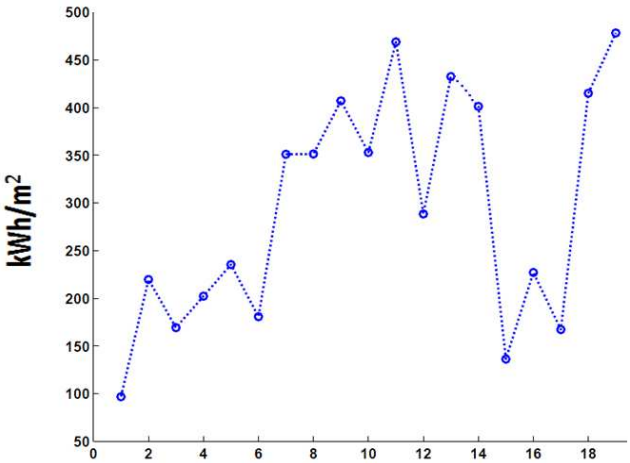

Fig. 8: The global solar energy per unit area variation for the last days of May 2008

Fig. 9 shows the experimental versus calculated H_c variation for the clearest day of May. It can be observed that the difference between the two series of data is small. In fact the Heliodon curve is a few percents smaller than the experimental one. This is due to diffuse radiation coming from the clear part of the sky, which is not considered in Heliodon.

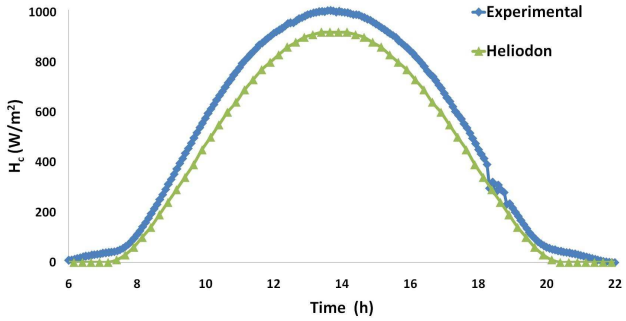

Fig. 9: Comparison between experimental and Heliodon' data for a sunny day

The total global radiation energy per unit area over all the period, obtained using the experimental device, was calculated and compared with the energy found using Heliodon for different inclination angles in order to find the optimum value for Compiègne. The results are presented in Table 1 for 30° (the actual angle), 39° and 60°. We should note that the table is prepared yearly. Figure 10 plots a comparison of the variation of the solar energy for 30°, 39° and 60° computed cases. The panel tilted at 60° receives more energy during winter and less during summer as expected. The 30° panel receives more energy in the summer, when the solar radiation is very high, and less in the winter compared with 60° panel. However, the peak was founded at 39° which is slightly different from the general rule used in the architecture for the optimal angle: latitude – 15°. However, it should be noted that this analysis is preliminary and further detailed analysis should be carried out.

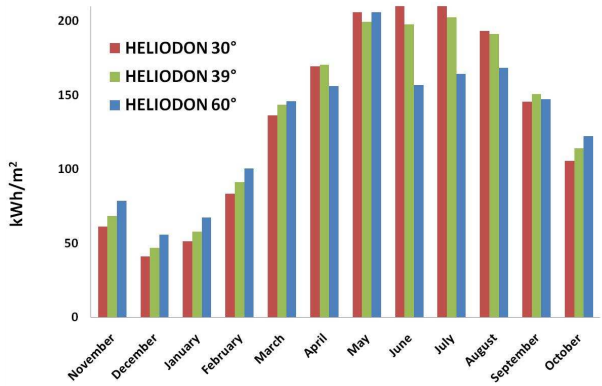

Fig. 10: Computed solar energy per unit area variation for different inclination angle

Table 1: The total energy for the full period

	Total (kWh / m^2)	**Day Average (kWh / m^2)**
Measured	1247.6	3.47
Heliodon 30°	1617.1	4.43
Heliodon 39°	1635.8	4.48
Heliodon 60°	1571.1	4.30

5 Correlation between Heliodon and experimental data

From the precedent section, the importance of a meteorological model able to modify the Heliodon data in order to obtain realistic simulation is clear. One of the most used methods to make this correlation is the simple empirical linear equation proposed by Angström in 1924 using experimental data from Stockholm [10]. The correlation, in its original form, was:

$$\frac{H}{H_0} = 0.25 + 0.75\,\frac{n}{N} \qquad (6)$$

where H and H_0 are the total irradiation income on horizontal surface for a day and for a perfectly clear sky, respectively while n/N is the time of sunshine expressed as the fraction of greatest possible time of sunshine. Since then, for the last 80 years, this equation was used in the same, similar and/or modified manner by many authors [11]. More details are given by Akinoglu in Badescu et al. [12].

The constants 0.25 and 0.75 are for Stockholm, and they are varying in a quite range of values for different locations. Therefore, it may be noteworthy to find some empirical constants for Compiegne using measured solar radiation.

In the reality, to find the empirical constants used in original Angström's equation or variations, we need specific experimental data. Generally, these kinds of data are not very common for many earth locations. So, we wanted to find another way to fit Heliodon with experimental data, first for Compiègne and later using the same methodology, for some other locations. This time we are using existing and very accessible kind of data.

Some public database, like SoDa [13], addresses the needs of industry and research for information on solar resource. On this site, we can obtain information about the annual frequency of the sunny, intermediate and cloudy skies. These parameters are calculated using satellite images and are available for many locations on

earth. The parameters for the city of Compiègne are listed in Table 2.

Table 2: Annual frequency of the sunny (S), intermediate (I) and cloudy (C) skies for Compiegne, France [13]:

Month	S (%)	I (%)	C (%)
January	29.4	41.6	29.1
February	27.4	41.4	31.2
March	32.7	39.1	28.2
April	36.3	37.5	26.2
May	36.8	38.2	25.0
June	36.6	37.6	25.8
July	35.3	41.4	23.4
August	46.8	38.3	14.9
September	43.8	37.3	18.9
October	34.6	39.3	26.1
November	27.0	47.3	25.8
December	23.2	46.0	30.8
Year	***34.2***	***40.4***	***25.4***

A linear equation based on the two parameters, was used to fit the experimental data and using the Heliodon results :

$$\frac{E_e}{E_H} = a + b \cdot S \qquad (7)$$

In this equation, E_e is the global solar radiation measured by the pyranometer, E_H is the clear sky solar radiation given by Heliodon. The regression coefficients, a, the constant term, and b, the slope of the equation, are found using the least square statistical method. In this equation, the frequency of intermediate and cloudy skies was not used in order to avoid some statistical problems, like multicollinearity [14]. All the possible linear equations, based on the three sky types (14 combinations for testing), have been tried. To see what model is statistically significant, some additional statistical indicators were used: adjusted R^2, F-test, t-statistic, like those defined in Walpole and Myers [15]. It has been observed that the t-statistic used in addition with some other statistical methods are giving more consistent results [16 - 18].

The best fitting results, from a statistical point of view, are presented on the Fig. 11. It may be noted that the experimental histogram and the Heliodon 30° histogram have the same aspect. The new total energy is 1255 kwh/m^2, less than 1% different from the measured one. This result shows the quality of the fitting process. The equation found for Compiègne is:

$$\frac{E_e}{E_H} = 0.313 + 1.252 \cdot S \qquad (8)$$

This parsimonious equation has a statistical indicator of correlation equal to R^2 = 0,58. The F Test for the equation and its parameters with a 95% of confidence is greater than the critic values. The sky frequency of sunny days (S) is a proxy variable [19] that is used in place of the sunshine duration used in the traditional Angström model (Angström, 1924). This might be used for a strong and positive correlation between these variables.

Finally, it can be seen that the equation (8) is similar with equation (6) proposed by Angström, but we should note that it is for inclined surface, and clear-sky value E_H is used instead of H_0. This is the reason why we have $E_e = 1.565 \cdot E_H$ for $S = 100\%$.

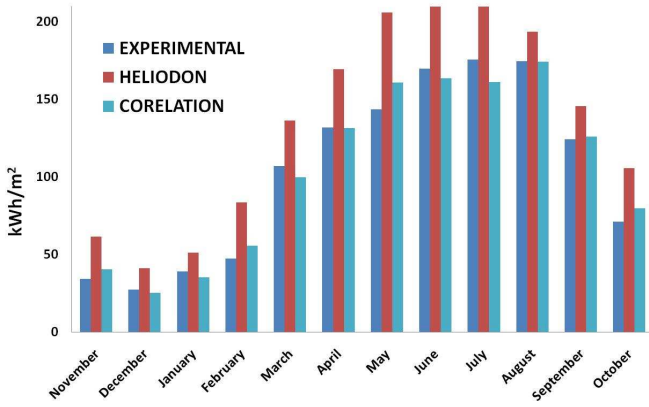

Fig. 11 Experimental vs Heliodon Data

In the equaton (7) is easy to analyse due to its univariate form and by evaluating in the extrems values we obtained that the quotient $\frac{E_e}{E_H}$ is between the limits of 60 and 90%.

Moreover, if we include the theoretical diffuse component [8, 20] to the beam radiation calculated by Heliodon, the model increases its statistical indicators but the complexity of the model also behaves as follows:

$$\frac{E_e}{E_H + E_D} = 2.04 \cdot S + 2.23 \cdot C - 1.82 \cdot I \qquad (9)$$

Here, E_D , is the theoretical diffuse solar radiation.

The positive sign of C is due to a the positive correlation between C and I (Figure 12 a). This indicates that the solar radiation decreases if C increases. In this equation (9) the statistical indicators mentioned before are better than in equation (8) and the R^2 = 0.87. The limits of the quotient are between 32 and 59%. The figure 12 shows the combinated impact of C and S, and it is clear that S has a positive impact in the equation and C and I have together a negative impact.

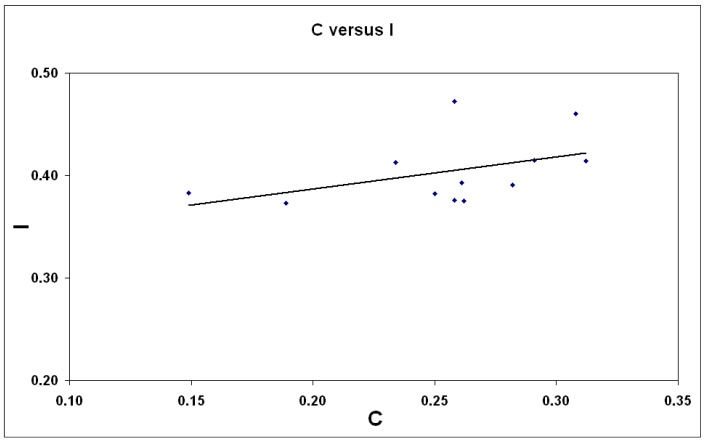

(a)

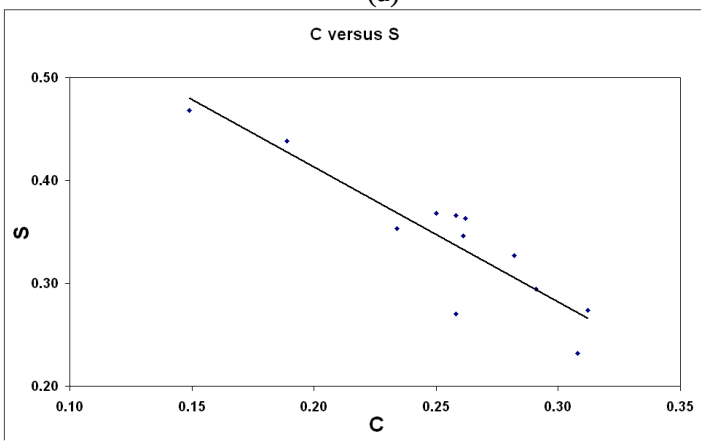

(b)

Fig. 12 C versus I and S

6 *In situ* measurements of the solar irradiance and comparison with Heliodon

First, the total and diffuse solar irradiance were measured in three different urban situations: a building terrace, a building court and a street. In the same time, another pyranometer was placed in an open area in order to have a clean comparison signal.

Second, the three cases were simulated using Heliodon software (figure 13).

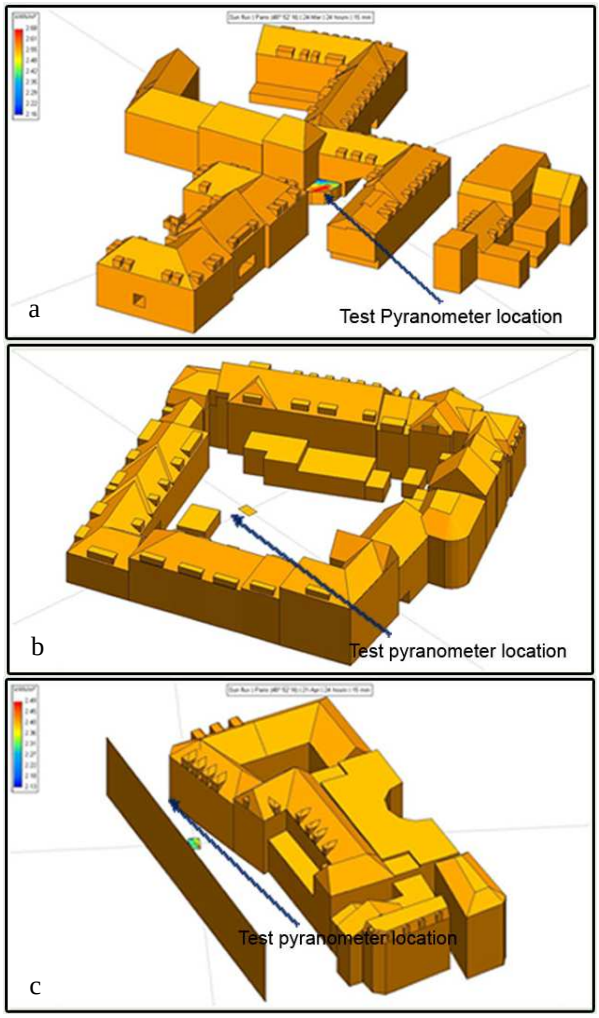

Fig. 13 Heliodon simulations of the building terrace (a), the building court (b) and the street (c)

A comparison between synchronized measurements with the two pyranometrs, in the same place, was carried out before to start the tests (figure 14).

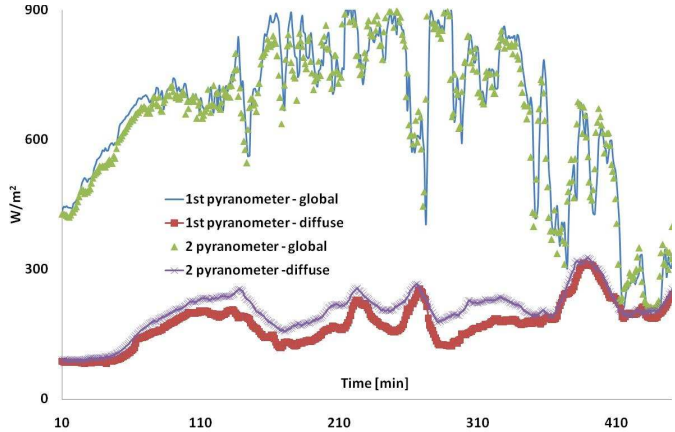

Fig. 14 Comparison between synchronized measurements with the two pyranometrs

Both pyranometers are able to measure the global and the diffuse solar radiation. The difference between the two pyranometers is small for the global solar radiation measurements and a little higher for the diffuse solar radiation measurements. However, we can see that the behaviors of the curves are similar for the two measurements so the same variation in the solar radiation will be detected.

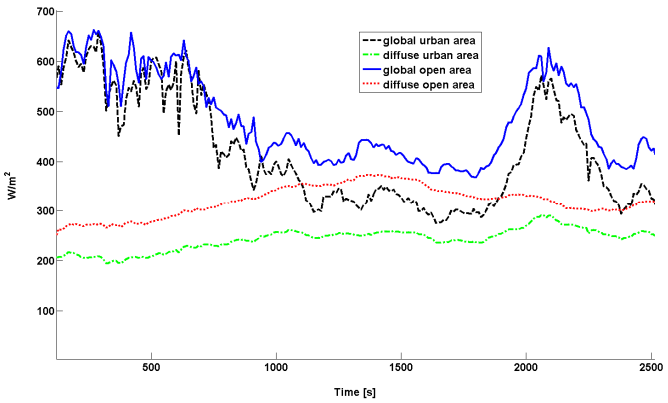

(a)

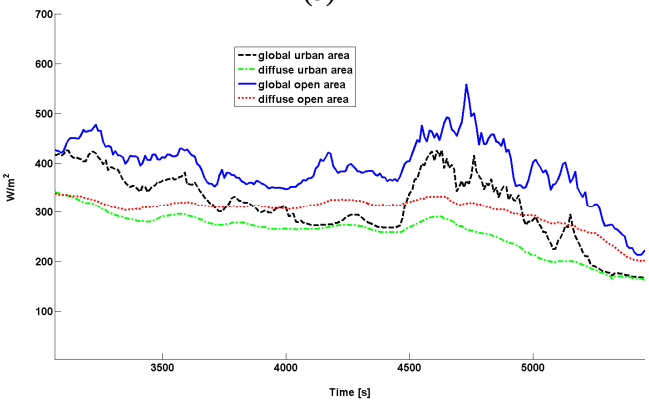

(b)

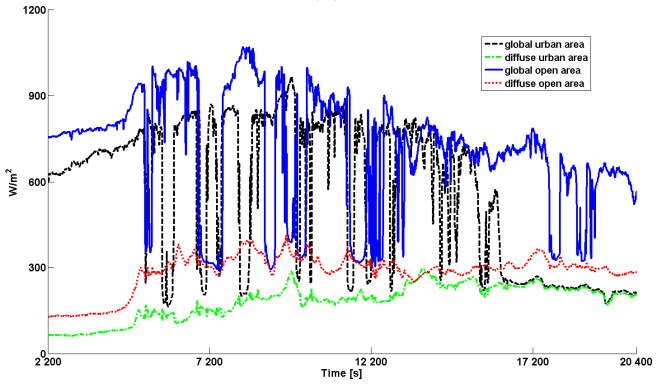

(c)

Fig. 15 Comparison between *in situ* measurements the open area measurements for the three test cases

First and second recordings were made, one after another, in the same day in two different places. During this day, the sky was generally cloudy. The third recording was made for a larger period of time in one place. The day was in-between, sunny periods alternating with totally overcast periods.

It is clear, from the figures, that the global and diffuse solar radiations are always smaller in the urban area than in the open area. On the other hand, there is no evidence of a direct coefficient of proportionality between the global flux measured in open and urban area. This is because many additional phenomena, like urban reflections, heat fluxes, convection, fluid dynamics…, will influence the measurements in an urban area.

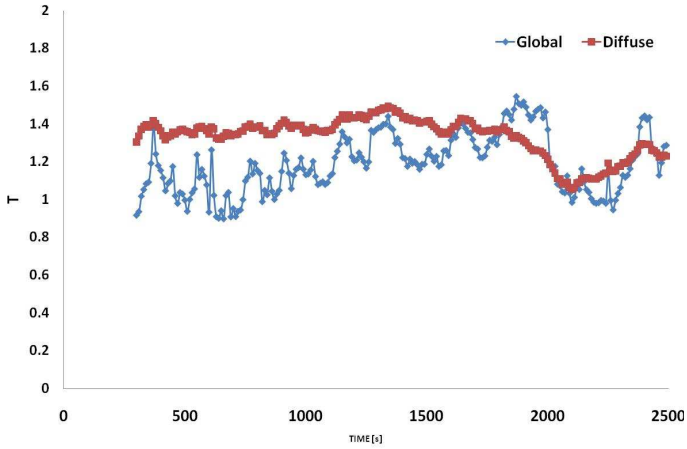

Fig. 16 Variation of the T coefficient for the first case

The diffuse solar radiation seems to be proportional during certain periods of time. This can be explained by the strong dependence of the diffuse solar radiation with the sky view factor, constant for a given position, and less dependent on the clouds variations. A variation of the proportionality coefficient defined like:

$$T = \frac{H_o}{H_u} \qquad (10).$$

Here H_o is the solar radiation measured in the open area and H_u is the solar radiation measured in the urban area for the first case is presented on the figure 16.

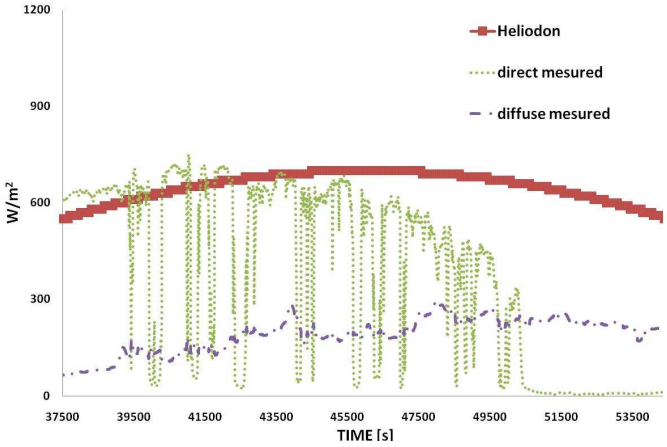

Fig. 17 *In situ* measurements versus Heliodon for the third case

The Figure 17 shows a comparison between the direct and diffuse flux measured in the third case and the Heliodon simulation. The direct solar radiation was calculated as the difference between the global and the diffuse radiation. As expected, we can see that the influence of the cloud is very important. The energy received over all the period is obtained by integrating the solar radiation. The results for the experimental case and Heliodon are presented in the table 3. Finally, the correlated energy is calculated using the equation 7. The relative error is smaller when we use the correlated value than the Heliodon one but the difference is not very important because the measured period is very small.

Table 3: The total energy for the third measured period

	Heliodon	**Experimental**	**Correlated**
Energy (kWh/m^2)	3.3	2.84	2.53
Error	16%	-	11%

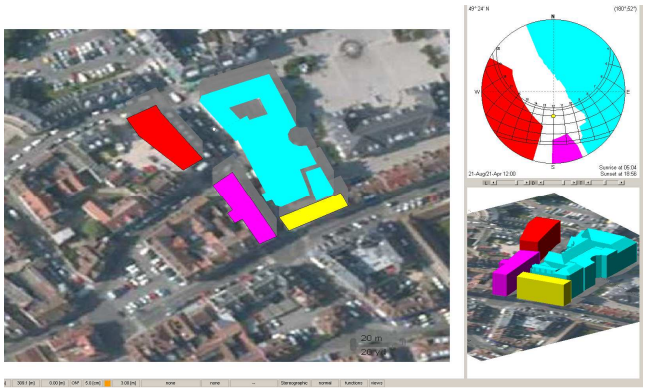

Fig. 18 Heliodon simulation of the third case

In the Figure 18, the complete Heliodon simulation of the third case is presented. Using the Heliodon software it is possible to analyze the evolution of the building mask over the test surface during the whole year. This information is synthesized on the stereographic projection (figure 18). For example, we can see that the blue building will shade the analyzed point during the whole year until 10 am and the red one on the afternoon starting at 01 pm in wintertime and at 03 pm in summertime. The pink building will mask the computation point during the winter from 11 am to noon. A comparison between the theoretical values of solar radiation received by a surface without masks (orange) and with the current masks (blue) is presented on the figure 19, with the solar irradiance above (a) and the total energy below (b).

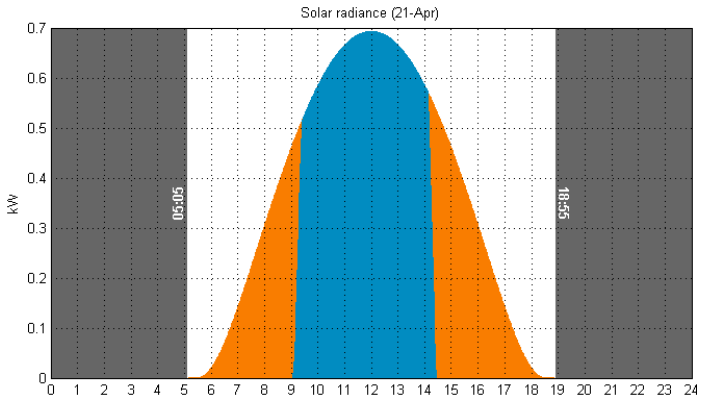

(a)

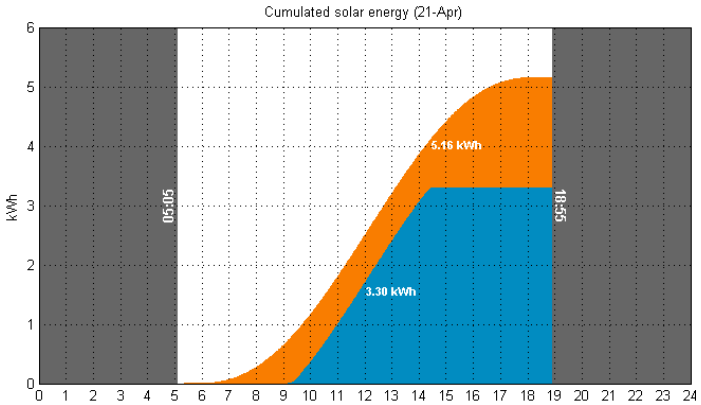

(b)

Fig. 19 No-shadowed solar radiation (orange) versus real solar radiation (blue)

7 Correction time for Compiegne

Heliodon is working with the solar time, which means that the sun crosses the meridian of the studied place exactly at noon. Transposed to GMT, the solar time of Compiègne (49° 24 N, 02° 50 E) must be decreased by the longitude of the city:

$$\frac{2 + \frac{5}{6}}{15} = 0.188888 \text{ hours} \qquad (11)$$

The legal time of Compiègne is GMT +1 (GMT +2 in summer). Solar noon corresponds to 00:48:36 pm in winter and 01.48:36 pm in summer. This result corresponds to a regular movement of the sun. In practice, it is necessary to add another correction of the time. It is due to the elliptic shape of the earth's orbit. By calculating the solution of Kepler's equation (equation of time), we can find the exact position of the sun at any time and thus its time of passage through the local meridian. The table, presented in appendix I, gives the time the sun moves across the meridian of Compiègne for a several days of the year and the correction C that has to be applied to the time displayed in Heliodon. For the other dates it is possible to perform a linear interpolation.

Summer: Legal time = Heliodon time + C + 2

Winter: Legal time = Heliodon time + C + 1 (12)

8 Conclusions and perspectives

This work shows that it is possible to correlate the results obtained from Heliodon, using only the direct sun flux, with the experimental results measured on an open surface. The tests were performed in Compiègne, France. The simple empirical equation may be used for a location close to Compiègne only by attributing the frequency of sunny days. However, it should be noted that it is derived for inclined surfaces with angle 30°. To improve the results a statistical analysis was done. Principally, t-statistic was used to evaluate the accuracy of the correlations described above.

It will be interesting to obtain different correlations for different seasons and for different locations from various climates. Nevertheless, this requires long term data on the earth surface measured by accurate instruments. A second step of this work will be to use the same methodology for data from some other locations and after that to see how the model works for non-free surfaces (shadowed ones) in a real urban situation.

References:

[1] L. Shashua-Bar, Built form thermal effects on the microclimate in the front and the rear open spaces of street buildings. Case study: Four archetypes of street buildings in the Mediterranean Sea coast region in summer, *WSEAS / IASME International Conference on Energy, Environment, Ecosystems and Sustainable Development*, Vouliagmeni, Athens, Greece, July 12-14, 2005

[2] Z. ZHANG, G. HE, A study on urban growth, vegetation space variation and thermal environmental changes of Beijing city based on TM imagery data, *2nd WSEAS International Conference on Remote Sensing*, Tenerife, Canary Islands, Spain, December 16-18, 2006

[3] M. Sechilariu, F. Locment, I. Houssamo, Production locale d'électricité renouvelable. Réseau semi-isolé et sécurisé pour bâtiments, *Conférence EF, ISBN 978-2-913923-30-0*, UTC, France 2009.

[4] K. Zakšek, T. Podobnikar and K. Oštir, Solar radiation modeling, *Computers & Geosciences*, Vol. 31, Issue 2, 2005, pp. 233-240.

[5] Heliodon 2 software and user's guide, B. Beckers & L. Masset, www.heliodon.net

[6] B. Beckers, L. Masset and P. Beckers, Enrichment of the visual experience by a wider choice of projections, *11th Intern. Conf. on Comp. Supported Cooperative Work in Design*, Australia 2007.

[7] B. Beckers, S D. Rodriguez, Helping architects to design their personal daylight, *WSEAS Transactions on Enviroment and Development*, Issue7, Vol.7, 2009, pp. 487-477.

[8] J. Campbell and M. Norman, *An introduction to Environmental Biophysics*, Springer, 1998

[9] B. Y. Liu, R. C. Jordan, The interrelationship and characteristic distribution of direct, diffuse, and total solar radiation, *Solar Energy,*, Vol. 4**,** 1960, pp. 1–19.

[10] A. Angström, Solar and terrestrial radiation, *Q.J.R Met. Soc.*, Vol. 50, 1924, pp. 121-126.

[11] A. G. K. Kostoulas G. A.Vokas, F. Skittides, Review of Solar Radiation estimation and Solar Data Banks elaboration methodologies over Greece, *WSEAS Transactions on Circuits and Systems*, Issue 5, Volume 3, 2004, pp. 1221-1227.

[12] B. G. Akinoglu, Recent Advances in the Relations between Bright Sunshine Hours and Solar Irradiation, *In: V. Badescu (ed.) - Modeling Solar Radiation at the Earth surface*, Springer, 2008, pp. 115-143.

[13] SoDa, Services for Professionals in Solar Energy and Radiation, *www.soda-is.com*.

[14] E.R Mansfield, B.P. Helms, Detecting multicollinearity, *Amer. Statist.*, Vol. 36**,** 1982, pp. 158–160.

[15] Walpole, R.E. and Myers, R.H. *Probability and statistics for engineers and scientists*. 4th ed. New York: Macmillan, 1989.

[16] R.J. Stone, Improved statistical procedure for the evaluation of solar radiation estimation models, *Solar Energy*, Vol. 51, 1993, pp. 289-299.

[17] I.T. Tögrul, Comparison of statistical performance of seven sunshine-based models for Elazığ, *Chimica Acta Turcica*, 1998, pp. 26-37.

[18] I.T. Tögrul, Estimation of solar radiation from Angström's coefficients by using geographical and meteorological data in Bishkek, Kyrgyztan, *J. of Thermal Science and Technology*, Vol. 29-2, 2009, pp. 99-108

[19] G. Upton, and I. Cook, (2002) *Oxford Dictionary of Statistics*, University Press, Great Britain.

[20] J. Duffie, and W. Beckman, (2006) *Solar Engineering of Thermal Processes*. Wiley. New Jersey

APPENDIX I

Day of the month	Month	Crossing the (GMT)meridian Decimal Time,	C = Correction, Decimals minutes
7	1	11.9173	-4.9617
14	1	11.9634	-2.1940
21	1	12.0006	0.0385
28	1	12.0275	1.6509
7	2	12.0468	2.8083
14	2	12.0472	2.8302
21	2	12.0376	2.2575
28	2	12.0195	1.1674
7	3	11.9943	-0.3447
14	3	11.9638	-2.1713
21	3	11.9300	-4.1982
28	3	11.8949	-6.3087
7	4	11.8460	-9.2426
14	4	11.8152	-11.0905
21	4	11.7890	-12.6590
28	4	11.7689	-13.8684
7	5	11.7533	-14.8009
14	5	11.7500	-15.0012
21	5	11.7543	-14.7399
28	5	11.7659	-14.0489
7	6	11.7925	-12.4483
14	6	11.8161	-11.0349
21	6	11.8414	-9.5190
28	6	11.8661	-8.0342
7	7	11.8936	-6.3820
14	7	11.9093	-5.4424
21	7	11.9182	-4.9057
28	7	11.9195	-4.8319
7	8	11.9070	-5.5797
14	8	11.8885	-6.6883
21	8	11.8628	-8.2341
28	8	11.8308	-10.1527
7	9	11.7771	-13.3740
14	9	11.7362	-15.8282
21	9	11.6946	-18.3222
28	9	11.6543	-20.7410
7	10	11.6075	-23.5525
14	10	11.5773	-25.3636
21	10	11.5545	-26.7280
28	10	11.5408	-27.5504
7	11	11.5394	-27.6370
14	11	11.5521	-26.8730
21	11	11.5763	-25.4215
28	11	11.6113	-23.3206
7	12	11.6699	-19.8036
14	12	11.7234	-16.5987
21	12	11.7805	-13.1680
28	12	11.8383	-9.7019